Effects of T142 Phosphorylation and Mutation R145G on the Interaction of the Inhibitory Region of Human Cardiac Troponin I with the C-Domain of Human Cardiac Troponin C†

Darrin A. Lindhout,‡ Monica X. Li,‡ Dean Schieve,§ and Brian D. Sykes*,‡

CIHR Group in Protein Structure and Function and Department of Biochemistry, University of Alberta, Edmonton, Alberta, Canada T6G 2H7

Received February 4, 2002; Revised Manuscript Received April 15, 2002

ABSTRACT: Cardiac troponin I (cTnI) is the inhibitory component of the troponin complex, and its interaction with cardiac troponin C (cTnC) plays a critical role in transmitting the Ca^{2+} signal to the other myofilament proteins in heart muscle contraction. The switch between contraction and relaxation involves a movement of the inhibitory region of cTnI (cIp) from cTnC to actin−tropomyosin. This region of cTnI is prone to missense mutations in heart disease, and a specific mutation, R145G, has been associated with familial hypertrophic cardiomyopathy. It also contains the unique cardiac PKC phosphorylation site at residue T142. To determine the structural consequences of the mutation R145G and the T142 phosphorylation on the interaction of cIp with cTnC, we have utilized 2D {^{1}H, ^{15}N}-HSQC NMR spectroscopy to monitor the binding of native cIp, cIp-R (R145G), and cIp-P (phosphorylated T142), respectively, to the Ca^{2+}-saturated C-domain of cTnC (cCTnC·2Ca^{2+}). We also report a strategy for cloning, expression, and purification of cTnI peptide, and both synthetic and recombinant peptides are used in this study. NMR chemical shift mapping indicates that the binding epitope of cIp on cCTnC·2Ca^{2+} is not greatly affected, but the affinity is reduced by ∼14-fold by the T142 phosphorylation and ∼4-fold by the mutation R145G, respectively. This suggests that these modifications of cIp have an adverse effect on the binding of cIp to cCTnC·2Ca^{2+}. These perturbations may correlate with the impairment or loss of cTnI function in heart muscle contraction.

The myofilament is the contractile machinery in cardiac muscle cells and plays a vital role in maintaining the normal function of heart. The contractile proteins include myosin, actin, tropomyosin, and troponin. Troponin is a 1:1:1 complex of troponin C, troponin I, and troponin T. During diastole, troponin holds tropomyosin in a conformational state that blocks the interaction between myosin and actin. When Ca^{2+} binds to troponin C during systole, the troponin−tropomyosin complex changes so that it no longer inhibits the interaction between actin and myosin. This leads to tension-producing cross bridges between actin and myosin, potentiating actomyosin ATPase activity, and ultimately heart muscle contraction [for recent reviews, see refs (*1, 2*)].

Cardiac troponin I (cTnI)[1] is the inhibitory component of the troponin complex, and its interaction with cardiac troponin C (cTnC) plays a critical role in transmitting the Ca^{2+} signal to the other myofilament proteins in heart muscle contraction. The solution structure of the Ca^{2+}-saturated cTnC has revealed a dumbbell molecule with two globular domains connected by a flexible linker (*3*). The solution structures of the N-domain of cTnC in both apo and Ca^{2+}-bound states have defined the Ca^{2+}-induced conformational transition in the regulatory domain of cTnC (*4*). Using the structure of cTnC as a framework, biochemical and biophysical studies have clarified how various regions of cTnI react with cTnC and participate in thin filament Ca^{2+}-signaling [for a review, see (*5*)]. An antiparallel arrangement between cTnC and cTnI has been proposed, and an inhibitory region has been identified [for a review, see (*5*)]. The so-called inhibitory region of cTnI is a 20 amino acid motif encompassing residues 128−147 in cTnI and corresponding to residues 96−115 in sTnI. This region is evolutionarily conserved and alternatively binds to either actin−tropomyosin or cTnC, depending on the intracellular concentration of Ca^{2+}. During diastole, when the $[Ca^{2+}]_i$ is low, the inhibitory region of cTnI bound strongly to actin−tropomyosin, inhibiting the power stroke. During systole, transient increases in $[Ca^{2+}]_i$ promotes Ca^{2+} binding to cTnC, facilitating a shift of this region of cTnI from the thin filament to cTnC. Thus, a movement of the inhibitory region of cTnI from cTnC to actin−tropomyosin constitutes the major switch between

† Supported by the Canadian Institutes of Health Research (CIHR) and the Heart and Stroke Foundation of Canada. D.A.L. is supported by an Alberta Heritage Foundation for Medical Research Studentship.

* To whom correspondence should be addressed. Phone: (780) 492-5460, Fax: (780) 492-0886, E-mail: brian.sykes@ualberta.ca.

‡ CIHR Group in Protein Structure and Function.

§ Department of Biochemistry.

[1] Abbreviations: TnC, troponin C; cTnC, human cardiac muscle TnC; sTnC, human skeletal muscle TnC; cCTnC, C-domain (90−161) of cTnC; sCTnC, C-domain (89−162) of sTnC; TnI, troponin I; cTnI, human cardiac muscle TnI; sTnI, human skeletal muscle TnI; cIp, synthetic inhibitory peptide Ac-cTnI$_{128-147}$-NH_2; cIp-P, synthetic inhibitory peptide Ac-cTnI$_{128-147}$-NH_2 with phosphorylation of T142; cIp-DL, recombinant inhibitory peptide NH_3^+-cTnI$_{128-147}$-hSer-CO_2-; cIp-R, recombinant inhibitory peptide NH_3^+-cTnI$_{128-147}$-hSer-CO_2- with mutation R145G; sIp, synthetic inhibitory peptide Ac-sTnI$_{96-115}$-NH_2; HSQC, heteronuclear single-quantum coherence; GB1, B1 immunoglobulin binding domain of streptococcal protein G.

10.1021/bi020100c CCC: $22.00
Published on Web 05/15/2002

muscle contraction and relaxation, and this switch is modulated by the interaction of the C-terminal domain of cTnI and cTnC (*6*, *7*). Structural data on cTnI include the early structure of the inhibitory peptide bound to cTnC determined by Campbell et al. (*8*) and the structural information generated by using NMR and selective isotope labeling on Met residues in both cTnC and cTnI (*9*−*14*). The NMR solution structure of the complex of the N-domain of cTnC and the cTnI 147−163 region is the only high-resolution structure of the cTnC−cTnI binary complex available to date (*15*). In this structure, the residues immediately following the inhibitory region of cTnI bind to the hydrophobic pocket of the N-domain of cTnC and stabilize its open conformation.

cTnI has many unique characteristics. The human cTnI is a 210 residue protein, and it differs from its skeletal isoform (sTnI) by a 33 amino acid N-terminal extension. There are also important sites of phosphorylation in cTnI that are not present in its skeletal counterpart. Two serine residues (serines 22 and 23), that are substrates for protein kinase A (PKA), lie within the N-terminal extension [for a review, see (*5*) and also (*12*, *16*)]. cTnI is also sensitive to protein kinase C (PKC) phosphorylation at serines 41 and 43, and at threonine 142 [for a review, see (*5*)]. The effect of cTnI phosphorylation is primarily a downward modulation of cardiac contractility, either by decreased atomyosin ATPase activity, which is mediated by PKC, or by increased binding of cTnI to the thin filament, mediated by PKA. cTnI is also implicated in various cardiac diseases. For example, familial hypertrophic cardiomyopathy, one of the most frequently occurring inheritated cardiac disorders, affecting up to 1 in 500 of the population, has been identified to be a sarcomere disease [for reviews, see (*17*, *18*)]. It is characterized by left ventricular hypertrophy, myofibril disarray, and sudden cardiac death and is believed to be caused by mutations in certain contractile protein genes, including cTnI. To date, six missense mutations (R145G, R145Q, R162W, S199N, G203S, and K206Q) on cTnI have been reported along with mutations causing the deletion of one codon (ΔK183) and a deletion of Exon8 (Δexon8) (*18*). Among those, R145G and R145Q are located in the key inhibitory region of cTnI. A truncation of cTnI has been associated with myocardial stunning (*19*, *20*), and measuring the serum level of cTnI has become the standard of care in the diagnosis of myocardial injury (*21*−*24*).

To understand how alterations in cTnI cause disease, it is important to elucidate the effects of cTnI modifications in its interaction with cTnC. In this report, we have evaluated the effects of T142 phosphorylation and mutation R145G on the interaction of the important inhibitory region of cTnI and cTnC. For the purpose of this study, we have chosen an isolated Ca^{2+}-saturated C-domain (residues 91−161) of human cTnC (cCTnC·$2Ca^{2+}$) since our earlier work has shown that the inhibitory peptide primarily interacts with the C-terminal domain of cTnC (*25*). The use of the smaller domain reduces the NMR spectral overlap and facilitates the assignment process. 2D {^{1}H,^{15}N} HSQC NMR spectroscopy was used to monitor the binding of native cIp, cIp-R (R145G), and cIp-P (T142 phophorylation), respectively, to cCTnC·$2Ca^{2+}$. Chemical shift mapping indicates that the binding epitope of cIp on cCTnC·$2Ca^{2+}$ is not greatly affected, but the affinity is reduced by ∼14-fold by the T142 phosphorylation and ∼4-fold by the mutation R145G, respectively. This suggests that even minor modifications of cIp can have an adverse effect on the binding of cIp to cCTnC·$2Ca^{2+}$. These perturbations may correlate with the impairment or loss of cTnI function in heart muscle contraction.

EXPERIMENTAL PROCEDURES

Sample Preparation. The engineering of the expression vector for the cCTnC (91−161) protein was as described in Chandra et al. (*26*). The expression and purification of ^{15}N-labeled protein in *Escherichia coli* follow the procedure as described previously for sNTnC (*27*), except a further purification step was done using a gravity flow Superdex 75 column (Amersham Pharmacia) with a buffer containing 150 mM NaCl and 50 mM Tris, pH 7.9. The protein was pooled and desalted on a Sephadex G25 (fine) column containing 10 mM NH_4HCO_3, pH 8.0, 0.01% (w/w) NaN_3, and was lyophilized to dryness. Three portions of ^{15}N-cCTnC were dissolved separately into 500 μL of NMR buffer containing 100 mM KCl, 10 mM imidazole in 90% H_2O/10% D_2O. The sample concentrations were determined to be 0.59, 0.40, and 0.24 mM, respectively, by amino acid analysis. To each sample was added 5 μL of 1 M $CaCl_2$ to ensure that the protein was Ca^{2+}-saturated, and the pH was adjusted to 6.7 by 1 M HCl and/or 1 M NaOH. Two synthetic peptides, acetyl-TQKIFDLRGKFKRP**T**LRRVR-amide, in both native (cIp) and T142-phosphorylated states (cIp-P), were prepared according to standard peptide synthetic procedures. Synthetic peptides were lyophilized twice to remove residual organic solvents. Solid cIp and cIp-P peptides were dissolved separately in NMR buffer containing 100 mM KCl, 10 mM imidazole (pH 6.7) in 90% H_2O/10% D_2O to make two stock solutions, with concentrations 45.1 and 16.6 mM, respectively, as determined by amino acid analysis.

Construction and Expression of cIp-DL and cIp-R Peptides. The construct of the recombinant cIp-DL peptide was produced as follows: the DNA region encoding residues 128−147 of human cTnI was obtained using primer 1 5′-CTAGCATGACCCAGAAAATTTTTGATCTGCGCGGCAAATTTAAACGCCCGACCCTGCGCGGCGTGCGCATGCCCCGCGGGCCCGGGC-3′ and primer 2 5′-TCGAGCCCGGGCCCGCGGGGCATGCGCACGCGGCGCAGGGTCGGGCGTTTAAATTTGCCGCGCAGATCAAAAATTTTCTGGGTCATG-3′. For recombinant cIp-R peptide, primer 3 5′-CTAGCATGACCCAGAAAATTTTTGATCTGCGCGGCAAATTTAAACGCCCGACCCTGCGCCGCGTGCGCATGCCCCGCGGCCCGGGC-3′ and primer 4 5′-TCGAGCCCGGGCCCGCGGGGCATGCGCACGCCGCGCAGGGTCGGGCGTTTAAATTTGCCGCGCAGATCAAAAATTTTCTGGGTCATG-3′ were used. Primers 1 and 2 and primers 3 and 4, respectively, were mixed to a final concentration of 50 nM in 50 μL of annealing buffer, 100 mM NaCl, and heated for 1 h at 100 °C and then allowed to cool to room temperature over 4 h. Annealed primers were precipitated by ethanol and incubated at − 20 °C for 30 min, followed by 13K centrifugation for 10 min, and then dissolved in TE buffer to a final concentration of 100 nM.

GEV-1 (*28*) vector was simultaneously digested with *Nhe*I and *Xho*I, and agarose gel purified using a Bio101 Geneclean

II kit. Using the *Nhe*I/*Xho*I sites, the ligated DNA insert products corresponding to cIp-DL and cIp-R, respectively, were cloned into the GEV-1 vector using a 3:1 insert-to-vector ratio. Following transformation into XL1 Blue *E. coli* cells and incubation at 37 °C on 2XYT/Amp plates, positive colonies were identified by *Sma*I digest, and labeled as GB1-cIp-DL and GB1-cIp-R, respectively.

E. coli BL21 DE3 (*pLysS*) cells were transformed with either GB1-cIp-DL or GB1-cIp-R and grown at 37 °C with shaking to $OD_{600} = 0.8$ in 2×YT media which contained 100 μg/mL ampicillin. Cultures were then induced with 1.2 mM isopropyl β-D-thiogalactoside (IPTG) and shaken at 37 °C for 4 h. To determine the extent of soluble expression, 1 L of culture was pelleted (centrifugation at 8K for 15 min) and lysed in a French pressure cell. Lysate was cleared by centrifugation (15K for 1 h) and analyzed by SDS−PAGE using the miniprotean III electrophoresis system (Biorad).

For large-scale preparation, BL21 DE3 (pLysS) cells which expressed GB1-cIp-DL or GB1-cIp-R were resuspended in 50 mM Tris, 5 mM EDTA, pH 8.0, and 0.01% (w/w) NaN_3, and broken in a French press cell. Following centrifugation, the supernatant was filtered through a 0.22 μm membrane prior to loading onto a 25 mL chelating Sepharose fast flow column (Amersham Pharmacia). Prior to protein loading, the column was charged with 50 mM $NiSO_4$ and equilibrated with 500 mM NaCl, 5 mM imidazole, 20 mM Tris-HCl, pH 7.9. After protein loading, the column was washed with 500 mM NaCl, 5 mM imidazole, 20 mM Tris-HCl, pH 7.9, followed by a further washing with 500 mM NaCl, 60 mM imidazole, 10 mM Tris-HCl, pH 7.9. Fusion proteins were eluted in 500 mM NaCl, 1 M imidazole, 10 mM Tris-HCl, pH 7.9. Eluted proteins were then desalted by loading on a Sephadex G-25 medium (Amersham Pharmacia) column in 10 mM NH_4HCO_3, pH 8.0, and lyophilized to dryness.

Fusion proteins were dissolved at 5 mg/mL in 0.1 M HCl, and CNBr was added to a final molar ratio of 100:1. Cleavage was allowed to progress for 24 h at room temperature, followed by 10-fold dilution in deionized water and lyophilized to dryness. cIp-DL and cIp-R were purified by HPLC, and the masses were verified by MALDI mass spectrometry. Pure cIp-DL and cIp-R fractions were collected and diluted by 2-fold in deionized water and twice lyophilized to dryness to remove any residual organic solvent. Unlike the synthetic peptide, the expressed peptide is not protected at both the N- and the C-terminal ends. Solid cIp-R peptide was dissolved in NMR buffer containing 100 mM KCl, 10 mM imidazole (pH 6.7) in 90% H_2O/10% D_2O to generate a stock solution of 14.0 mM as determined by amino acid analysis.

1D ^{1}H NMR spectroscopy was used to check the result of CNBr cleavage of the GB1-cIp-DL fusion protein. 3.5 mg of solid GB1-cIp-DL was dissolved into 500 μL of NMR buffer containing 100 mM KCl, 10 mM imidazole (pH 6.7) in 90% H_2O/10% D_2O. Peaks corresponding to Met residues (ϵ-CH_3) were monitored to determine quantitative cleavage by CNBr.

Titration of ^{15}N-cCTnC·2Ca^{2+} with cIp. To an NMR tube containing a 500 μL sample of 0.59 mM ^{15}N-cCTnC·2Ca^{2+} were added aliquots of 1.8 μL of 45.1 mM cIp stock solution for the first 5 titration points. Aliquots of 1.9 μL were added for the next 7 titration points, followed by aliquots of 4.9 μL for the next 3 titration points, followed by a final addition of 9 μL to ensure complete cIp saturation. The sample was thoroughly mixed after each addition. After every titration point, 1 μL of the resulting titrated solution was removed and used for amino acid analysis. The change in cCTnC·2Ca^{2+} concentration due to increased volume during the titration was taken into account for data analysis; the change in pH for cIp addition was negligible. Both 1D ^{1}H and 2D {^{1}H, ^{15}N}-HSQC spectra were acquired at every titration point. To check if the synthetic (cIp) and recombinant (cIp-DL) peptides bind the same way to cCTnC·2Ca^{2+}, 8.1 mg of solid cIp-DL was added to a 0.92 mM ^{15}N-cCTnC·2Ca^{2+} sample to generate the complex cCTnC·2Ca^{2+}·cIp-DL, in which the $[\text{cIp-DL}]_{total}/[\text{cCTnC·2Ca}^{2+}]_{total}$ is ∼5:1, corresponding to the final ratio for the $[\text{cIp}]_{total}/[\text{cCTnC·2Ca}^{2+}]_{total}$ complex. The 2D {^{1}H, ^{15}N}-HSQC spectrum was acquired and superimposed with that of the cCTnC·2Ca^{2+}·cIp complex.

Titration of ^{15}N-cCTnC·2Ca^{2+} with cIp-P. To an NMR tube containing a 500 μL sample of 0.40 mM ^{15}N-cCTnC were added aliquots of 1 μL of 16.6 mM cIp-P stock solution for the first 12 titration points. Aliquots of 2 μL were added for the next 2 titration points, followed by aliquots of 3 μL for 3 titration points, and two additions of 4 μL to ensure complete cIp-P saturation. The sample was thoroughly mixed after each addition. After every titration point, 1 μL of the resulting titrated solution was removed and used for amino acid analysis. The change in cCTnC·2Ca^{2+} concentration due to increased volume during the titration was taken into account for data analysis; the change in pH for cIp-P addition was negligible. Both 1D ^{1}H and 2D {^{1}H, ^{15}N}-HSQC spectra were acquired at every titration point.

Titration of ^{15}N-cCTnC·2Ca^{2+} with cIp-R. To an NMR tube containing a 500 μL sample of 0.29 mM ^{15}N-cCTnC were added aliquots of 1 μL of 14.9 mM cIp-R stock solution for the first 9 titration points. Aliquots of 2 μL were added for the next 2 titration points, followed by additions of 3, 5, and 7 μL to ensure complete cIp-R saturation. The sample was thoroughly mixed after each addition. After every titration point, 1 μL of the resulting titrated solution was removed and used for amino acid analysis. The change in cCTnC·2Ca^{2+} concentration due to increased volume during the titration was taken into account for data analysis; the change in pH for cIp-R addition was negligible. Both 1D ^{1}H and 2D {^{1}H, ^{15}N}-HSQC spectra were acquired at every titration point.

NMR Spectroscopy. All of the NMR spectra were obtained using a Unity INOVA 500 MHz spectrometer at 30 °C. All 1D ^{1}H NMR spectra were acquired with a sweep width of 6000 Hz with 128 transients, respectively. All 2D {^{1}H, ^{15}N}-HSQC spectra were acquired using the sensitivity-enhanced gradient pulse scheme developed by Lewis E. Kay and coworkers (*29*, *30*). The ^{1}H and ^{15}N sweep widths were 7000 and 1500 Hz, with 16 transients and 128 increments, respectively. Spectral processing and analyses were accomplished with the programs NMRPipe (*31*) and NMRview (*32*), respectively. The chemical shift mapping technique was used to delineate the binding sites of the cIp peptides on the structure of cCTnC·2Ca^{2+}. This approach has been demonstrated to be extremely useful for quickly identifying general sites of interaction between protein and ligand (*25*, *33*−*35*).

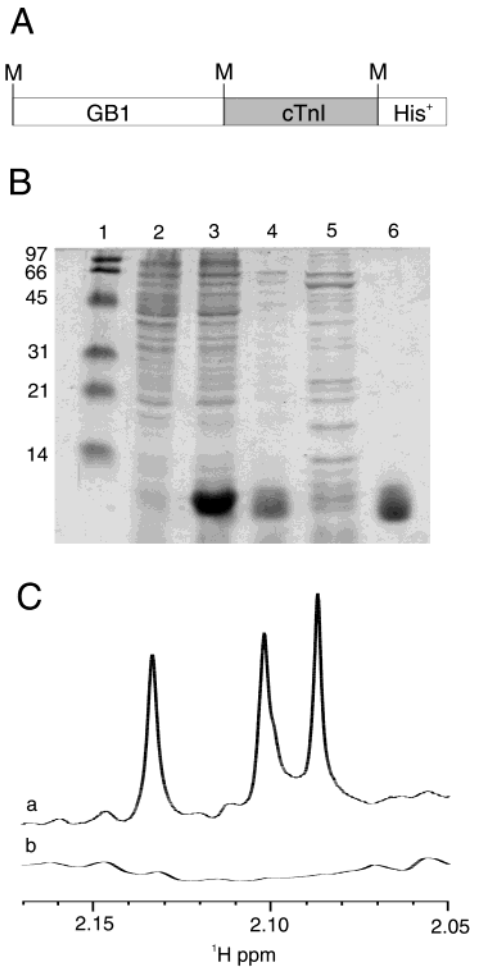

FIGURE 1: (A) GB1-cIp-DL fusion protein construct. M indicates the location of methionine residues. (B) SDS−PAGE of Bio-Rad low molecular weight markers (lane 1), GB1-cIp-DL uninduced (lane 2) and induced (lane 3) cells, soluble supernatant following French press lysis (lane 4), column flow-throw following loading on a Ni^{2+} affinity column (lane 5), and purified GB1-cIp-DL (lane 6). (C) ^1H NMR spectrum of GB1-cIp-DL prior to (a) and after (b) CNBr cleavage.

RESULTS

Expression of cIp-DL in E. coli. We have established a strategy for expressing and purifying the inhibitory region of cTnI peptide, cIp-DL, based on the method by Huth et al. (*28*). The construct used to generate the cIp-DL peptide is shown in Figure 1A. Figure 1B shows the 15% SDS−PAGE gel for the expression and purification of GB1-cIp-DL. As can be seen in lane 3, the induced cells express a dark band at approximately 11 kDa, which is the expected molecular mass of the fusion protein (10 937.8 Da). The fusion protein is in the soluble fraction following French press and subsequent centrifugation. Lane 6 shows the purifed GB1-cIp-DL following purification on a chelating Sepharose flow-through column. Expression yields approximately 80 mg of lyophilized GB1-cIp-DL protein per liter of induced 2×YT media. Expression of GB1-cIp-R yields identical expression and purification results (data not shown). Figure 1C shows a region of the 1D ^1H NMR spectra of GB1-cIp-DL prior to and after CNBr cleavage, respectively. Three singlet peaks from the three Met residues (ϵ-CH_3) are present in the uncleaved GB1-cIp-DL fusion protein at 2.09, 2.10, and 2.13 ppm, respectively, representing the N-terminal Met and the two Met residues on the N- and C-terminus of the cIp-DL insert. Upon CNBr cleavage, the peaks have disappeared, indicating complete digestion of GB1-cIp-DL fusion protein. Identical results were seen for GB1-cIp-R fusion protein (data not shown). Following HPLC purification of cleaved GB1-cIp-DL, MALDI mass spectrometry yielded 5 peaks. One peak at 1547.6 Da corresponds to the cleaved C-terminal His tag which has a predicted molecular mass of 1547.7 Da. Two peaks at 2617.5 and 2599.5 Da correspond to the cleaved cIp-DL peptide with a C-terminal homoserine and homoserine lactone, respectively, which have predicted molecular masses of 2618.2 and 2600.2 Da. Two peaks at 6544.5 and 6564.5 Da correspond to the cleaved N-terminal GB1 protein with a C-terminal homoserine and homoserine lactone, respectively, which have predicted molecular masses of 6534.2 and 6554.2 Da.

Effect of cIp, cIp-P, and cIp-R on cCTnC·2Ca²⁺. The titration of ^{15}N-cCTnC·$2Ca^{2+}$ with cIp, cIp-P, and cIp-R, respectively, as monitored by 2D {^1H, ^{15}N}-HSQC NMR spectral changes is shown in Figure 2. The 2D {^1H, ^{15}N}-HSQC NMR spectrum of cCTnC·$2Ca^{2+}$ is completely assigned and was used as a starting point to monitor the cIp peptide-induced chemical shift changes. Comparison of the three panels in Figure 2 immediately suggests that all three peptides induce the same pattern of backbone amide resonance changes of cCTnC·$2Ca^{2+}$. Typical examples are G140, I128, and T129. All of the chemical shift changes fall into the fast exchange limit on the NMR time scale. Linear movement of cross-peaks indicates that only two species exist and the binding occurs with a 1:1 stoichiometry in the interaction between cCTnC·$2Ca^{2+}$ and the respective cIp peptide. Each cross-peak position corresponds to the weighted average of the bound and free chemical shifts of cCTnC·$2Ca^{2+}$.

Resonances which undergo backbone amide ^1H and/or ^{15}N chemical shift changes during titration were followed to monitor peptide binding to protein. For cIp titration, the peptide-induced chemical shift changes of individual amide resonances as a function of the $[cIp]_{total}/[cCTnC{\cdot}2Ca^{2+}]_{total}$ ratio was plotted, and the average curve is shown in Figure 3A. The normalized average chemical shift data as a function of $[cIp]_{total}/[cCTnC{\cdot}2Ca^{2+}]_{total}$ were fit to the equation:

$$cCTnC{\cdot}2Ca^{2+} + cIp \leftrightarrow cCTnC{\cdot}2Ca^{2+}{\cdot}cIp$$

which yielded a dissociation constant (K_D) of 31 ± 11 μM. Similar procedures were applied to the titrations with cIp-P and cIp-R, and the binding curves are shown in Figure 3B and 3C, respectively. The determined dissociation constants are 451 ± 10 μM for cIp-P and 122 ± 17 μM for cIp-R, respectively. This suggests that the binding affinity of cIp for cCTnC·$2Ca^{2+}$ is reduced ~14-fold by the T142 phosphorylation and ~4-fold by the mutation R145G.

Inspection of Figure 2 shows different degrees of chemical shift changes for different residues in cCTnC·$2Ca^{2+}$. For example, residues such as I128 and V160 undergo large chemical shift perturbations, indicating potential contacts with cIp, whereas residues such as I112 and D113 show relatively small cIp-induced chemical shifts. Thus, it is useful to correlate peptide-induced chemical shift changes to residues along the cCTnC·$2Ca^{2+}$ protein sequence. Figure

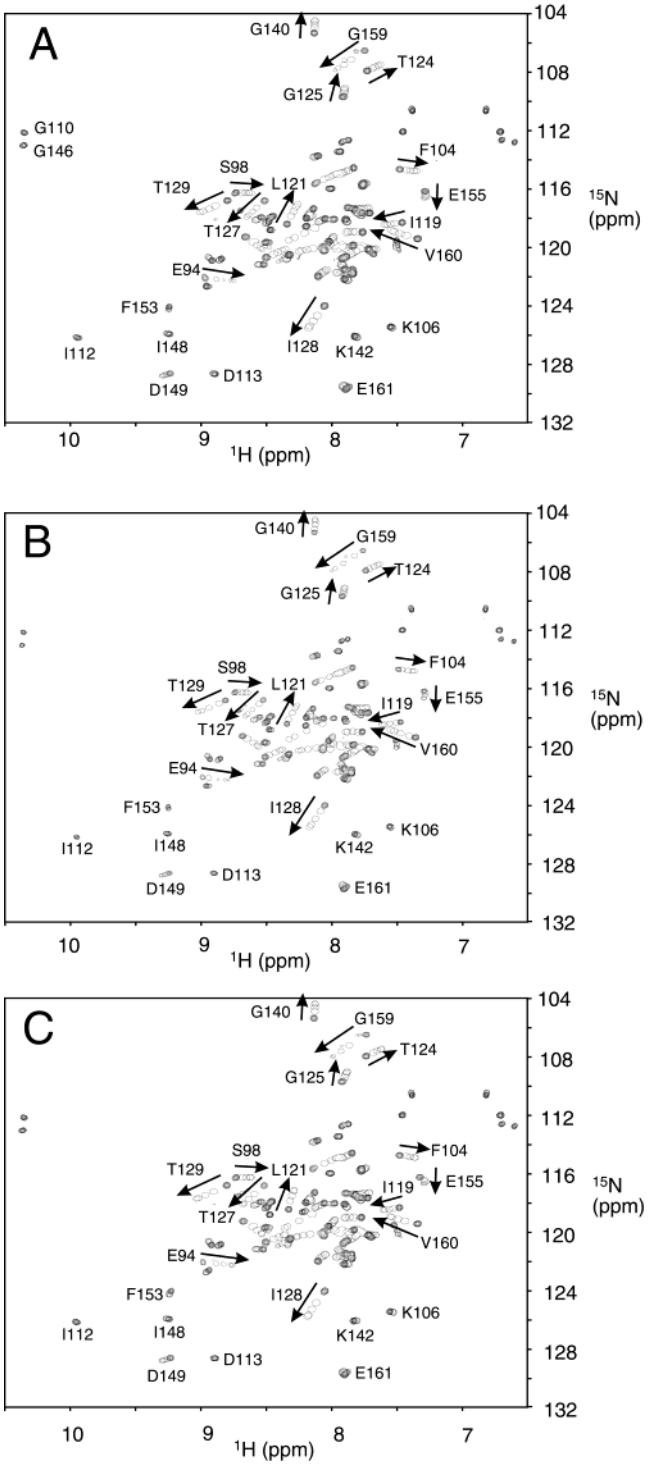

FIGURE 2: Titration of ^{15}N-cCTnC·2Ca^{2+} with (A) cIp, (B) cIp-P, and (C) cIp-R. 2D {^{1}H, ^{15}N}-HSQC NMR spectra from the backbone amide regions of cCTnC (●) at various concentrations of (A), (B), and (C), are superimposed (○), showing the progressive shifts of peaks. In all panels, the directions of the chemical shift changes for some residues undergoing large perturbations are indicated by an arrow. Conditions are as described under Experimental Procedures.

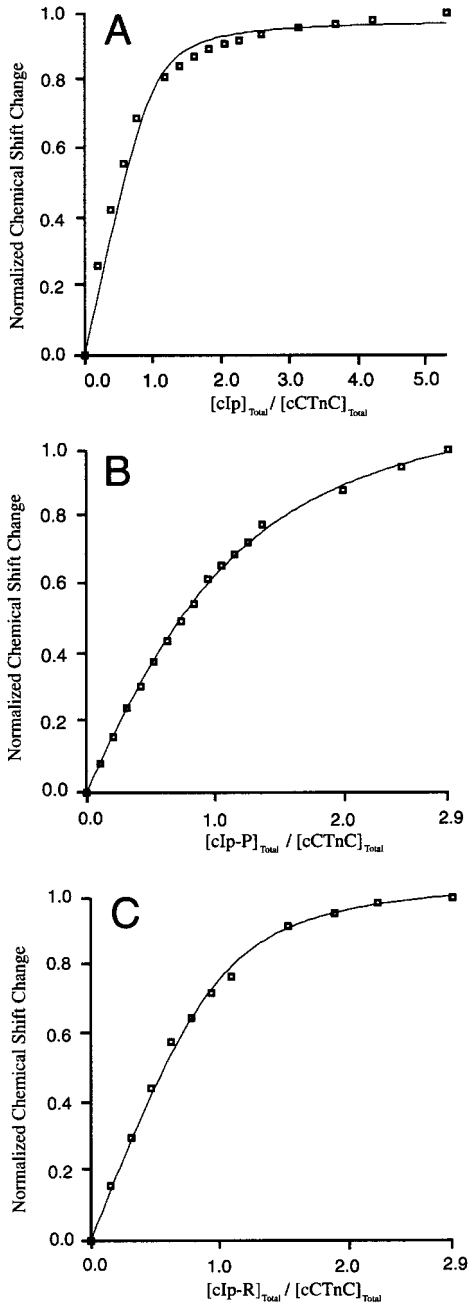

FIGURE 3: Titration of cCTnC·2Ca^{2+} with (A) cIp, (B) cIp-P, and (C) cIp-R. The curve for each panel represents the average of all residues followed in Figure 2A−C. The curves are normalized according to $(\delta_{obs} - \delta_{initial})/(\delta_{complex} - \delta_{initial})$. The best-fit curve to the data is shown by a solid line. Conditions are as described under Experimental Procedures.

4A plots the absolute chemical shift changes in both ^{1}H and ^{15}N dimensions against the protein sequence with different colors coding three cIp peptides. The important point of this plot is that the patterns induced by three peptides are very similar although to a slightly different extent. This plot shows that many residues experience significant peptide-induced chemical shift perturbations ($\Delta\delta_{ppm}$ > 0.5 ppm). Mapping of these residues on the surface of the structure of cCTnC·2Ca^{2+} reveals a broad binding surface for cIp (Figure 4B), which closely resembles that obtained in the interaction of cIp and intact cTnC·3Ca^{2+} (*25*). Similar binding surfaces were obtained when the chemical shift mapping was performed with cIp-P or cIp-R peptides (data not shown). This result shows clearly that the binding epitope of cIp on cCTnC·2Ca^{2+} is not greatly affected by either the T142 phosphorylation or the mutation R145G although its affinity for cCTnC·2Ca^{2+} is altered dramatically, especially a greater than 10-fold decrease with the T142 phosphorylation.

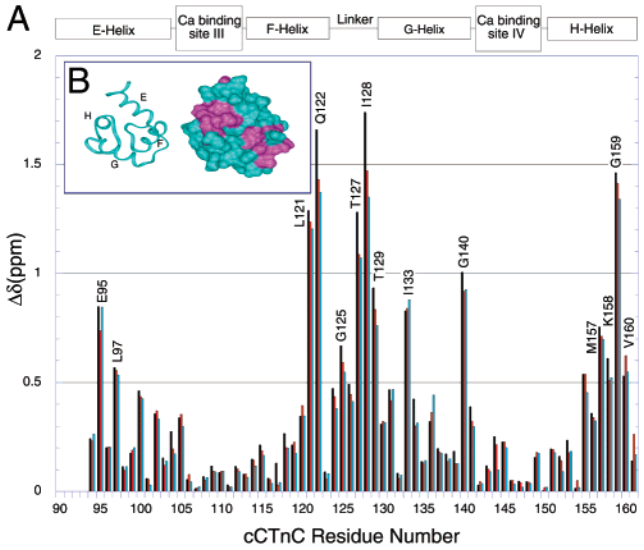

FIGURE 4: (A) Comparison of induced chemical shift changes of cCTnC·Ca^{2+} upon the addition of cIp-R (black), cIp-P (red), and cIp (blue). The orientation of the cCTnC protein backbone is shown as a ribbon diagram. (B) To show the extent of the total chemical shift changes ($\Delta\delta_{total}$) of cCTnC upon peptide binding, the $\Delta\delta_{total}$ of cIp binding (Figures 2A, 3A, and 4, black) was used to illustrate plausible binding to the surface of cCTnC. A view of the figure after a 180° rotation along the *y* axis does not show an interaction with cIp on the other side of cCTnC. Residues undergoing total chemical shift changes greater than one-half standard deviation of the average of all residues ($\approx \overline{\Delta\delta_{total}} + \sigma/2$) are colored in purple.

To determine if the expressed peptide cIp-DL binds in the same manner as the synthetic peptide cIp, the complex cCTnC·$2Ca^{2+}$·cIp-DL was generated, and the 2D {^{1}H, ^{15}N}-HSQC spectrum performed on the complex (data not shown) superimposes precisely with that of a cCTnC·$2Ca^{2+}$·cIp complex with no noticeable changes. This indicates that neither the N-terminus acetylation and the the C-terminus amide in the synthetic cIp nor the homeserine and homoserine lactone groups in the recombinant cIp-DL affect the binding of cIp to cCTnC·$2Ca^{2+}$.

DISCUSSION

The role of myofilament contractile proteins in heart diseases is just beginning to be recognized. Recent studies have identified various myofilament protein modifications correlated with cardiac dysfunction [for reviews, see (*17, 18*)]. cTnI is one of the intensively modified proteins found in diseased heart. For example, multiple mutations in cTnI have been associated with familial hypertrophic cardiomyopathy, an autosomal dominant disease of the sarcomere. Two mutations are located in the important inhibitory domain of cTnI (residues 128−147), a highly conserved region that alternatively binds either to actin−tropomyosin in muscle relaxation or to cTnC in muscle contraction. cTnI is also found to undergo posttranslational modifications by phosphorylation and proteolysis. The effect of cTnI phosphorylation is primarily a downward modulation of cardiac contractility (*5*), and a truncation of cTnI has been associated with myocardial stunning (*19, 20*). Although many functional and animal model experiments have revealed the functional differences between native and altered cTnI that may underlie the pathogenesis of cardiac disease (*20, 36*−*40*), there are few data available concerning the structural consequences of the alteration in the interaction of either cTnI with cTnC or cTnI with actin−tropomyosin. In this report, we focus on investigating the effects of T142 phosphorylation and mutation R145G on the interaction of the inhibitory region of human cTnI and the Ca^{2+}-saturated C-domain of human cTnC by the use of 2D {^{1}H, ^{15}N}-HSQC NMR spectroscopy.

We first examined the binding of cIp peptide to cCTnC·$2Ca^{2+}$, and this titration is used as a basis for evaluating the binding of the modified peptides, cIp-P and cIp-R. The dissociation constant for cIp binding to cCTnC·$2Ca^{2+}$ is 31 ± 11 μM. This affinity is comparable to that of sIp for sCTnC·$2Ca^{2+}$ (K_D = 47 μM) (*41*). However, it is ~2.5-fold stronger than that observed in the binding of cIp to intact cTnC·$3Ca^{2+}$ (*25*). One rationalization for this difference may be that the flexible central linker between the two globular domains of cTnC (*3*) allows the N-domain to bend over and interact with the C-domain, similar to that observed in the X-ray structure of sTnC·$2Ca^{2+}$·$sTnI_{1-47}$ (*42*). This may partially block the binding of cIp to the C-domain of cTnC and thereby lessen the affinity of cIp for cTnC. The epitope of cIp on cCTnC·$2Ca^{2+}$ as presented here is strikingly similar to that of cIp on cTnC·$3Ca^{2+}$, and the binding site for cIp consists of discrete patches on the surface of cCTnC·$2Ca^{2+}$ (see Figure 4B). This agrees with our previous conclusion (*25*) that the bound inhibitory region of cTnI adopts an extended conformation that stretches across the hydrophobic surface of the C-domain of cTnC·$3Ca^{2+}$. It is necessary to put our result into perspective with other available information on the inhibitory region of cTnI. To date, it is still under debate about where the inhibitory region of cTnI binds to cTnC. In recent sTnC−sTnI models, the inhibitory region interacts with the central helix area (including part of the D-helix in the N-domain and part of the E-helix in the C-domain of cTnC). One model suggests a β-hairpin structure (*43*) while another proposes an α-helical version (*44*). In the recent 2.6 Å resolution X-ray structure of cTnC·$3Ca^{2+}$·$cTnI_{34-210}$·$cTnT2_{182-288}$ (*45*), the structure and the binding site of the inhibitory region remain undefined. Our results on the interaction of cIp−cTnC·$3Ca^{2+}$, cIp−cCTnC·$2Ca^{2+}$, and sIp−sCTnC·$2Ca^{2+}$ strongly suggest that a binding site for the inhibitory region of TnI primarily resides on the C-domain of TnC. Interestingly, this binding epitope is not greatly perturbed by either the T142 phosphorylation or the mutation R145G, indicating the binding orientation of cIp on cCTnC·$2Ca^{2+}$ is not affected by these alterations. However, its affinity for cCTnC·$2Ca^{2+}$ is perturbed dramatically, i.e., a ~14-fold reduction by phosphorylation of T142 and a ~4-fold reduction by mutation of R145G.

T142 is a cardiac-specific residue (P110 in sTnI) located in the highly evolutionarily conserved inhibitory region of cTnI and is the substrate of protein kinase C (PKC). The functional consequence of this modification is the depressed ATPase activity and contractility (*5*). This is not surprising in light of our observation that the T142 phosphorylation reduced the affinity of the inhibitory region of cTnI for cTnC by ~14-fold. Since the interaction of cIp and cTnC constitutes the critical switch for transmitting the Ca^{2+} signal to the rest of the myofilament proteins, our results strongly suggest that T142 phosphorylation in cTnI modulates the Ca^{2+} regulation of contraction by impairing the interaction of cIp and cTnC, which may contribute to depressed ATPase activity and contractility.

The functional implication of mutation R145G in cardiac disease has been studied extensively since it was first reported in 1997 as a familial hypertrophic cardiomyopathy-causing mutation (*46*). This mutation constitutes a change in charge in an evolutionary conserved residue located in the important inhibitory region of cTnI. The functional abnormalities revealed reduced ability to inhibit actomyosin ATPase and an increase in Ca^{2+} sensitivity of actomyosin ATPase regulation (*36*, *37*, *39*, *40*). If these functional differences manifest themselves in vivo, there will be impairment of relaxation of cardiac muscle, and this altered contractility may provide a hypertrophic stimulus leading to the diseased state. This is proven by a mouse model study that shows that at the whole organ level, contractile function is enhanced but relaxation is compromised (*38*). Because cTnI binds to both cTnC and actin, it seems likely that that the primary etiology of cardiac dysfunction in the cTnI mutant R145G lies in altered cTnI interactions with cTnC, actin, or both. The binding of the inhibitory domain of cTnI to actin inhibits actomyosin ATPase activity, depresses cross-bridge cycling, and prevents contraction. The inhibition is released as cTnI binding shifts from actin to cTnC, an action favored by an increase in $[Ca^{2+}]_i$ during systole, when Ca^{2+} binds to the N-domain of cTnC. Thus, it seems that cTnI (R145G) either does not interact appropriately with actin or perhaps binds strongly to cTnC. The net effect would be the lack of the actomyosin ATPase inhibition. However, our present results indicate that the affinity of cIp for cCTnC·$2Ca^{2+}$ is reduced ~4-fold by the mutation R145G. It is possible that this mutation reduces the affinity of cIp for actin even more. The end result would be an imbalance of power between the competing actin and cTnC for cIp. This is conceivable since in heart cells, the myofilament proteins work in a highly organized and cooperative manner and the precision of the protein−protein interactions is controlled by a delicate energetic balance [see discussions in (*47*)]. Any subtle alterations would be expected to disrupt the harmony and cause functional anomalies.

Another important outcome of this report is that we have demonstrated the viable expression and purification of peptide fragments for use in NMR. Previous studies have relied on the use of synthetic peptides, which have limitations on synthesis length and product yield. We have obtained a very high yield of GB1-cIp-DL and GB1-cIp-R fusion proteins (80 mg each from 1 L of 2×YT media, respectively), which are highly soluble in contrast to many peptide-fusion systems. As GB1-cIp-DL and GB-1-cIp-R lack Met residues in the sequence of the inserted peptide, the use of CNBr in cleavage is of great importance as it allows GB1-cIp-DL and GB1-cIp-R to be expressed and cleaved with only an amino group and homoserine on the N- and C-termini. Future work with possible Met-rich peptide-fusion constructs may need to be designed to have enzymatic cut sites present on the N- and C-termini of the inserted peptide, as CNBr would lead to peptide fragmentation. Enzymatic cleavage may be hazardous to the activity and binding of the peptide as numerous residues may remain on the N- and C-termini of the cleaved peptide. Also, enzymatic cleavage of fusion proteins may not yield 100% cleavage, leading to lower than predicted peptide yield and possible troubles in later peptide purification. CNBr cleavage of GB1-cIp-DL has been shown to be quantitative. As has been discussed, the presence of a homoserine on the C-terminus of cIp-DL does not alter its binding for cCTnC·$2Ca^{2+}$. Although all peptides discussed in this paper were not expressed to contain isotopic labeling, expression of GB1-cIp-DL and GB1-cIp-R in ^{13}C- and/or ^{15}N-labeled media would yield labeled peptides, which can then be advantageously used in numerous heteronuclear NMR experiments to supplement current homonuclear peptide experiments, a project currently in progress in our laboratory.

Conclusions. This study was undertaken to investigate the interaction of cCTnC with the inhibitory region of cTnI in native, T142 phosphorylated, and mutation R145G states. Detailed titrations monitored by 2D {^1H, ^{15}N}-HSQC NMR spectroscopy reveal that the cIp peptides in native or modified states all bind to cCTnC·$2Ca^{2+}$ in 1:1 ratios. Chemical shift mapping indicates that the binding epitope of cIp on cCTnC·$2Ca^{2+}$ is not greatly affected, but the affinity is reduced by ~14-fold by T142 phosphorylation and ~4-fold by mutation R145G, respectively. This suggests that even minor modifications of cIp can have an adverse effect on the binding affinity of cIp for cCTnC·$2Ca^{2+}$. These perturbations may correlate with the impairment or loss of cTnI function in heart muscle contraction.

ACKNOWLEDGMENT

We gratefully acknowledge Dr. G. Marius Clore and coworkers (National Institutes of Health, Bethesda, MD) for the kind gift of the GEV-1 vector and for helpful discussions. We are indebted to Drs. R. John Solaro and Murali Chandra (University of Illinois−Chicago) for providing the cCTnC construct and Mr. David Corson and Ms. Angela Thiessen for assistance with the protein expression. We thank Mr. Paul Semchuck and Mr. Lorne Burke for assistance with HPLC purification and MALDI mass spectrometric measurements and Mr. Gerry McQuaid for spectrometer maintenance. We also thank Dr. Michael A. Geeves (University of Kent at Canterbury) for helpful discussions.

REFERENCES

1. Geeves, M. A., and Holmes, K. C. (1999) *Annu. Rev. Biochem. 68*, 687−728.
2. Gordon, A. M., Homsher, E., and Regnier, M. (2000) *Physiol. Rev. 80*, 853−924.
3. Sia, S. K., Li, M. X., Spyracopoulos, L., Gagné, S. M., Liu, W., Putkey, J. A., and Sykes, B. D. (1997) *J. Biol. Chem. 272*, 18216−18221.
4. Spyracopoulos, L., Li, M. X., Sia, S. K., Gagné, S. M., Chandra, M., Solaro, R. J., and Sykes, B. D. (1997) *Biochemistry 36*, 12138−12146.
5. Solaro, R. J., and Rarick, H. M. (1998) *Circ. Res. 83*, 471−480.
6. Rarick, H. M., Tu, X. H., Solaro, R. J., and Martin, A. F. (1997) *J. Biol. Chem. 272*, 26887−26892.
7. Ramos, C. H. (1999) *J. Biol. Chem. 274*, 18189−18195.
8. Campbell, A. P., and Sykes, B. D. (1991) *J. Mol. Biol. 222*, 405−421.
9. Krudy, G. A., Kleerekoper, Q., Guo, X., Howarth, J. W., Solaro, R. J., and Rosevear, P. R. (1994) *J. Biol. Chem. 269*, 23731−23735.
10. Howarth, J. W., Krudy, G. A., Lin, X., Putkey, J. A., and Rosevear, P. R. (1995) *Protein Sci. 4*, 671−680.
11. Kleerekoper, Q., Howarth, J. W., Guo, X., Solaro, R. J., and Rosevear, P. R. (1995) *Biochemistry 34*, 13343−13352.
12. Finley, N., Abbott, M. B., Abusamhadneh, E., Gaponenko, V., Dong, W., Gasmi-Seabrook, G., Howarth, J. W., Rance, M., Solaro, R. J., Cheung, H. C., and Rosevear, P. R. (1999) *FEBS Lett. 453*, 107−112.

13. Abbott, M. B., Gaponenko, V., Abusamhadneh, E., Finley, N., Li, G., Dvoretsky, A., Rance, M., Solaro, R. J., and Rosevear, P. R. (2000) *J. Biol. Chem. 275*, 20610−20617.
14. Abbott, M. B., Dvoretsky, A., Gaponenko, V., and Rosevear, P. R. (2000) *FEBS Lett. 469*, 168−172.
15. Li, M. X., Spyracopoulos, L., and Sykes, B. D. (1999) *Biochemistry 38*, 8289−8298.
16. Gaponenko, V., Abusamhadneh, E., Abbott, M. B., Finley, N., Gasmi-Seabrook, G., Solaro, R. J., Rance, M., and Rosevear, P. R. (1999) *J. Biol. Chem. 274*, 16681−16684.
17. Redwood, C. S., Moolman-Smook, J. C., and Watkins, H. (1999) *Cardiovasc. Res. 44*, 20−36.
18. Hernandez, O. M., Housmans, P. R., and Potter, J. D. (2001) *J. Appl. Physiol. 90*, 1125−1136.
19. McDonough, J. L., Arrell, D. K., and Van Eyk, J. E. (1999) *Circ. Res. 84*, 9−20.
20. Murphy, A. M., Kogler, H., Georgakopoulos, D., McDonough, J. L., Kass, D. A., Van Eyk, J. E., and Marban, E. (2000) *Science 287*, 488−491.
21. D'Costa, M., Fleming, E., and Patterson, M. C. (1997) *Am. J. Clin. Pathol. 108*, 550−555.
22. Van Eyk, J. E., Powers, F., Law, W., Larue, C., Hodges, R. S., and Solaro, R. J. (1998) *Circ. Res. 82*, 261−271.
23. McDonough, J. L., Labugger, R., Pickett, W., Tse, M. Y., MacKenzie, S., Pang, S. C., Atar, D., Ropchan, G., and Van Eyk, J. E. (2001) *Circulation 103*, 58−64.
24. Lee, T. H., and Goldman, L. (2000) *N. Engl. J. Med. 342*, 1187−1195.
25. Li, M. X., Spyracopoulos, L., Beier, N., Putkey, J. A., and Sykes, B. D. (2000) *Biochemistry 39*, 8782−8790.
26. Chandra, M., Dong, W. J., Pan, B. S., Cheung, H. C., and Solaro, R. J. (1997) *Biochemistry 36*, 13305−13311.
27. Li, M. X., Gagné, S. M., Tsuda, S., Kay, C. M., Smillie, L. B., and Sykes, B. D. (1995) *Biochemistry 34*, 8330−8340.
28. Huth, J. R., Bewley, C. A., Jackson, B. M., Hinnebusch, A. G., Clore, G. M., and Gronenborn, A. M. (1997) *Protein Sci. 6*, 2359−2364.
29. Kay, L. E., Keifer, P., and Saarinen, T. (1992) *J. Am. Chem. Soc. 114*, 10663−10665.
30. Zhang, O., Kay, L. E., Olivier, J. P., and Forman-Kay, J. D. (1994) *J. Biomol. NMR 4*, 845−858.
31. Delaglio, F., Grzesiek, S., Vuister, G. W., Zhu, G., Pfeifer, J., and Bax, A. (1995) *J. Biomol. NMR 6*, 277−293.
32. Johnson, B. A., and Blevins, R. A. (1994) *J. Biomol. NMR 4*, 603−614.
33. Shuker, S. B., Hajduk, P. J., Meadows, R. P., and Fesik, S. W. (1996) *Science 274*, 1531−1534.
34. Sun, C., Cai, M., Gunasekera, A. H., Meadows, R. P., Wang, H., Chen, J., Zhang, H., Wu, W., Xu, N., Ng, S. C., and Fesik, S. W. (1999) *Nature 401*, 818−822.
35. Medek, A., Hajduk, P. J., Mack, J., and Fesik, S. W. (2000) *J. Am. Chem. Soc.*, 1241−1242.
36. Takahashi-Yanaga, F., Morimoto, S., and Ohtsuki, I. (2000) *J. Biochem. (Tokyo) 127*, 355−367.
37. Elliott, K., Watkins, H., and Redwood, C. S. (2000) *J. Biol. Chem. 275*, 22069−22074.
38. James, J., Zhang, Y., Osinska, H., Sanbe, A., Klevitsky, R., Hewett, T. E., and Robbins, J. (2000) *Circ. Res. 87*, 805−811.
39. Takahashi-Yanaga, F., Morimoto, S., Harada, K., Minakami, R., Shiraishi, F., Ohta, M., Lu, Q. W., Sasaguri, T., and Ohtsuki, I. (2001) *J. Mol. Cell. Cardiol. 33*, 2095−2107.
40. Deng, Y., Schmidtmann, A., Redlich, A., Westerdorf, B., Jaquet, K., and Thieleczek, R. (2001) *Biochemistry 40*, 14593−14602.
41. Mercier, P., Li, M. X., and Sykes, B. D. (2000) *Biochemistry 39*, 2902−2911.
42. Vassylyev, D. G., Takeda, S., Wakatsuki, S., Maeda, K., and Maeda, Y. (1998) *Proc. Natl. Acad. Sci. U.S.A. 95*, 4847−4852.
43. Tung, C. S., Wall, M. E., Gallagher, S. C., and Trewhella, J. (2000) *Protein Sci. 9*, 1312−1326.
44. Luo, Y., Wu, J. L., Li, B., Langsetmo, K., Gergely, J., and Tao, T. (2000) *J. Mol. Biol. 296*, 899−910.
45. Takeda, S., Yamashida, A., Maeda, K., and Maeda, Y. (2002) *Biophys. J. 82*, 170a.
46. Kimura, A., Harada, H., Park, J. E., Nishi, H., Satoh, M., Takahashi, M., Hiroi, S., Sasaoka, T., Ohbuchi, N., Nakamura, T., Koyanagi, T., Hwang, T. H., Choo, J. A., Chung, K. S., Hasegawa, A., Nagai, R., Okazaki, O., Nakamura, H., Matsuzaki, M., Sakamoto, T., Toshima, H., Koga, Y., Imaizumi, T., and Sasazuki, T. (1997) *Nat. Genet. 16*, 379−382.
47. McKay, R. T., Saltibus, L. F., Li, M. X., and Sykes, B. D. (2000) *Biochemistry 39*, 12731−12738.

BI020100C